

Temperature-dependent valence-band photoemission study of UNiSn

J.-S. Kang

Department of Physics, The Catholic University of Korea, Puchon 420-743, Korea

J.-G. Park

Department of Physics, Inha University, Incheon, Korea

K. A. McEwen

Department of Physics and Astronomy, University College London, WC1E 6BT, United Kingdom

C. G. Olson

Ames Laboratory, Iowa State University, Ames, Iowa 50011

S. K. Kwon and B. I. Min

Department of Physics, Pohang University of Science and Technology, Pohang 790-784, Korea

(Received 18 February 2001; published 11 July 2001)

The electronic structure of UNiSn has been investigated using photoemission spectroscopy (PES). The U $5f$ partial spectral weight (PSW) exhibits a broad peak centered at ≈ 0.3 eV below E_F . The Ni $3d$ PSW shows the main peak well below E_F and a very low density of states (DOS) at E_F . The $h\nu$ dependence of the valence-band spectrum reveals a dominant U $5f$ electron character for the states near the Fermi level E_F , with a small contribution from the U $6d$, Ni $3d$, and Sn sp states. Comparison of the measured PES spectra to the LSDA+ U band structure calculation indicates the importance of the on-site Coulomb interaction between U $5f$ electrons in UNiSn. The high-resolution photoemission spectrum of UNiSn is described well by a V-shaped metallic DOS near E_F , suggesting a finite but reduced DOS at E_F . A possible origin for the reduced DOS at E_F might be the hybridization of the U $5f$ states to the Ni $3d$ states that have a very low DOS at E_F . T -dependent high-resolution PES for UNiSn reveals a finite DOS at E_F even above T_N .

DOI: 10.1103/PhysRevB.64.085101

PACS number(s): 79.60.-i, 71.20.Eh, 71.27.+a

I. INTRODUCTION

UNiSn displays an interesting phase transition. Powder neutron diffraction¹ and magnetic susceptibility^{2,3} show that an antiferromagnetic (AF) order of type I is formed below the Néel temperature $T_N \approx 43$ K. Temperature- (T -) dependent electrical resistivity $\rho(T)$ exhibits an activation-type T dependence above 200 K with an energy gap of 67–76 meV, a maximum around 55 K, and a rapid decrease with decreasing T ,^{3,4} indicating a semiconductor-to-metal (SM) transition. Recent powder x-ray diffraction reveals a structural transition from a cubic MgAgAs-type symmetry to tetragonal symmetry at T_N .⁵ This phase transition is considered to be anomalous because it is an inverse metal-insulator transition with a gap opening above T_N and the structural, SM, and AF transitions occur concomitantly.

UNiSn has been extensively investigated to understand the underlying mechanism of the peculiar multiple phase transitions. Aoki *et al.* explained⁶ the AF and structural transition using a crystal electric field (CEF) level scheme for the $5f^2$ (U^{4+}) configuration in a cubic symmetry. This model was supported by Akazawa *et al.*⁷ who proposed the existence of a quadrupolar-ordered phase from resistivity, elastic moduli, susceptibility, and thermal expansion studies. Indeed quadrupolar ordering has been indicated in high-resolution neutron inelastic scattering,⁸ in accordance with the above hypothesis.⁷ These models assume the localized $5f$ electrons in UNiSn in the CEF, which is consistent with the general

consensus of strongly correlated U $5f$ electrons in heavy-fermion uranium intermetallic compounds.

On the other hand, there is no indication of heavy-electron behavior in UNiSn. For example, the specific heat coefficient of UNiSn is quite modest, $\gamma \approx 18$ – 28 mJ/mol K², suggesting a moderate $5f$ electron density of states (DOS) at the Fermi level E_F .^{2,6} The electronic structure of UNiSn has been calculated by incorporating the on-site Coulomb interactions of $5f$ electrons,⁹ and the magnetic phase transition in UNiSn is explained as due to a reconstruction of the bands. It has also been suggested that the hybridization between the Sn p and U f and that between the Ni d and U f are important in determining the physical properties of UNiSn.⁶

Neither the theoretically predicted electronic structure of UNiSn nor the $5f^2$ configuration of the localized U^{4+} ion has been verified by photoemission spectroscopy (PES). There is an early resonant photoemission spectroscopy (RPES) study on UTSn ($T = \text{Ni, Pd, Pt}$) with a rather poor instrumental resolution,¹⁰ in which the origin of the phase transitions in UNiSn has not been addressed. Further, no T -dependent PES study on UNiSn has been reported yet to our knowledge. Therefore the expected gap opening or reduction in the DOS at E_F $N(E_F)$ in the semiconducting phase above T_N , as compared to the metallic phase at low T , has not been experimentally observed. In order to investigate the role of the electronic structure in the phase transitions in UNiSn, we have performed high-resolution T -dependent PES measurements of UNiSn below and above $T_N \approx 43$ K. We

have also performed a detailed RPES study of UNiSn near the U $5d \rightarrow 5f$ absorption edge, which allows us to determine the partial spectral weight (PSW) distributions of both U $5f$ and Ni $3d$ electrons in UNiSn. Experimental data are compared to a band structure calculation performed in the local spin-density functional approximation (LSDA) and the LSDA+ U method (U is the Coulomb correlation interaction).¹¹

II. EXPERIMENTAL AND CALCULATIONAL DETAILS

For this work, we prepared a large button of UNiSn polycrystalline sample by arc melting constituent elements of high purity. In order to ensure homogeneity of the sample, we turned over the button several times during the arc melting process. Afterwards we annealed the button at 1070 K for 1 month in order to achieve a cubic MgAgAs-type structure. Our magnetization measurements taken on the sample after 1 month annealing showed a clear antiferromagnetic transition near 48 K, in agreement with previous results.³

Photoemission experiments were carried out at the Ames/Montana ERG/Seya beam-line at the Synchrotron Radiation Center. Samples were cooled down to $T_{msr} \leq 15$ K and fractured in vacuum with a base pressure better than 3×10^{-11} Torr. The cleanliness of the cleaved surfaces was checked by the absence of the 6 eV peak (Ref. 12) or a hump at about 9.5 eV binding energy (BE), as observed sometimes in inhomogeneous polycrystalline samples.¹³ The Fermi level and the overall instrumental resolution of the system were determined from the valence-band spectrum of a sputtered Pt foil. The total instrumental resolution [full width at half maximum (FWHM)], due to both the monochromator and the electron energy analyzer, was about 80 meV and 250 meV at $h\nu \sim 20$ eV and $h\nu \sim 100$ eV, respectively. High-resolution photoemission spectra were taken with the FWHM of about 30 meV. The photon flux was monitored by the yield from a gold mesh and all the spectra reported were normalized to the mesh current. For T -dependent PES measurements, the chamber pressure stayed below 7×10^{-11} Torr during heating. The low- T PES spectra were reproduced after the heating-cooling cycle.

The electronic structure of UNiSn has been calculated by employing the self-consistent linearized muffin-tin-orbital (LMTO) band method. The projected angular momentum density of states (PLDOS) has been calculated by using both the LSDA and LSDA+ U methods. The von Barth–Hedin form of the exchange-correlation potential has been utilized. In the LSDA+ U method, the spin-orbit interaction is incorporated in a self-consistent variational loop, so that the orbital polarization is properly taken into account.¹⁴

III. RESULTS AND DISCUSSION

A. U $5f$ PSW and valence-band features

Figure 1 shows the valence-band energy distribution curves (EDC's) of UNiSn in the photon energy ($h\nu$) range of 22–110 eV, which includes both the Ni $3p$ and U $5d$ absorption thresholds. The variation in the line shape with varying $h\nu$ reflects the change in the photoionization matrix elements

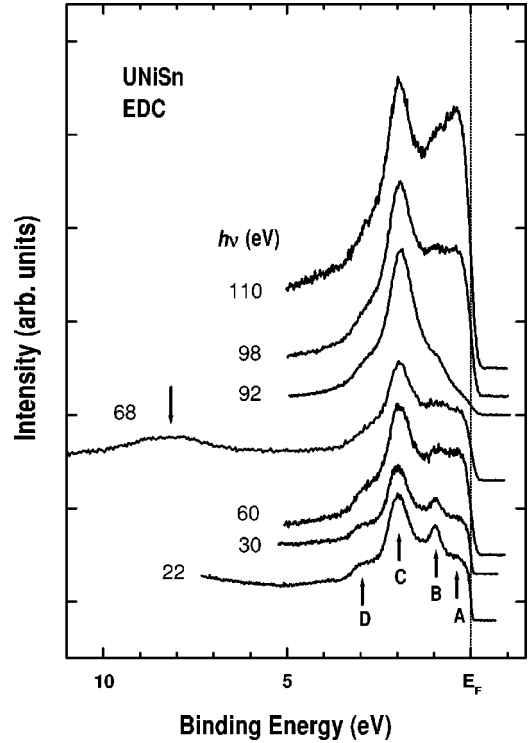


FIG. 1. Normalized valence-band energy distribution curves (EDC's) of UNiSn in the photon energy ($h\nu$) range of 22–110 eV, except for the $h\nu=22$ and 30 eV spectra that are arbitrarily scaled to show their line shapes better. The peak under the arrow at $h\nu=68$ eV corresponds to the Ni $3d$ satellite. See the text for the structures of A, B, C, and D.

with $h\nu$. Here $h\nu=98$ and $h\nu=92$ eV correspond to the on- and off-resonance energies due to U $5d_{5/2} \rightarrow 5f$ absorption, respectively,¹⁵ and $h\nu=110$ eV is another on-resonance energy due to U $5d_{3/2} \rightarrow 5f$ absorption. Therefore the emission enhanced at $h\nu=98$ and $h\nu=110$ eV can be identified as due to U $5f$ emission, and the strong enhancement in the emission between E_F and about 1.5 eV in binding energy indicates the large U $5f$ electron character in the electronic states close to E_F . This will be discussed further in Fig. 2.

The off-resonance spectrum at $h\nu=92$ eV is dominated by Ni $3d$ emission because at this $h\nu$ the Sn sp electron emission is negligible with respect to the Ni $3d$ emission ($<1\%$ of the Ni $3d$ emission),¹⁶ and the U $5f$ emission is suppressed due to off resonance. The latter argument is supported by the fact that the off-resonance spectrum of UNiSn is very similar to that of CeNiSn (Ref. 17) except for the Ni $3d$ peak position: the Ni $3d$ peak in UNiSn is located deeper than that in CeNiSn by about 0.5 eV. Similarly as in Ni metal,¹⁸ the main peak around 2 eV BE and the satellite peak around 8 eV BE (6 eV below the main peak) in the $h\nu \sim 68$ eV spectrum can be roughly assigned to the $3d^n c^{m-1}$ and $3d^{n-1} c^m$ final states, respectively, by assuming the initial state configuration of $3d^n c^m$ ($n=9,10$) where c denotes a conduction or ligand electron. This assignment of the satellite is based on the observation that the Ni $3d$ satellite emission is resonantly enhanced at $h\nu=68$ eV in Ni $3p \rightarrow 3d$ RPES.¹⁷ The satellite structure associated with the Ni

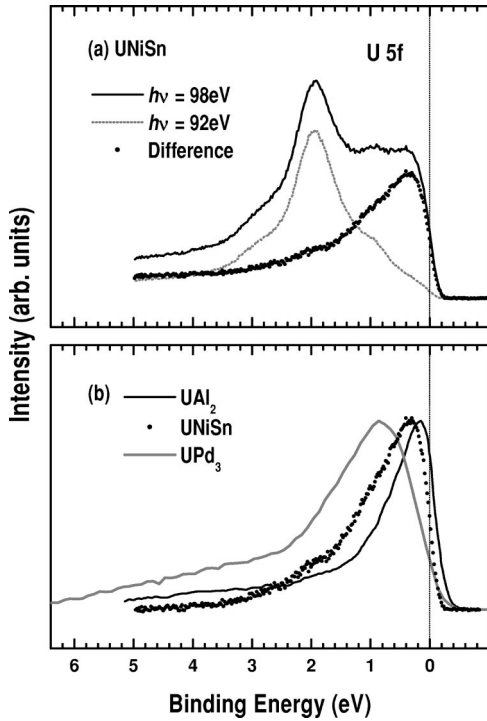


FIG. 2. (a) The extracted U $5f$ spectrum (dots) of UNiSn, obtained from subtraction of the U $5d \rightarrow 5f$ off-resonance spectrum (dashed lines) from the on-resonance spectrum (solid lines). (b) Comparison of the U $5f$ PSW's of UNiSn, UAl_2 (from Ref. 20), and UPd_3 (from Ref. 22).

$3d$ bands, not explained by one-electron band theory, reflects the non-negligible on-site Coulomb interaction between the Ni $3d$ electrons in UNiSn.

At low $h\nu$'s (22–30 eV), four structures are observed, labeled as A near E_F , B (~ 1 eV), C (~ 2 eV), and a weak shoulderlike structure D (~ 3 eV). These well-separated structures, the absence of the 6 eV BE feature,¹² and the low inelastic background indicate the good quality of the data in this work. At these low $h\nu$'s, the cross sections (σ) of U $6d$ and Ni $3d$ electrons become comparable to one another with non-negligible contributions from the Sn sp electrons:

$$\begin{aligned} \sigma(\text{U } 5f) : \sigma(\text{U } 6d) : \sigma(\text{Ni } 3d) : \sigma(\text{Sn } sp) \\ \approx 6\% : 41\% : 41\% : 12\% \quad \text{at } h\nu \approx 21 \text{ eV,} \end{aligned}$$

according to the atomic photoionization cross-section calculation.¹⁶ Therefore the valence-band spectra at low $h\nu$'s indicate that the U $6d$ and Sn sp states in UNiSn are spread over the whole valence band, i.e., from E_F to ~ 4 eV below. The features A and C are mostly due to the U $5f$ electrons and the Ni $3d$ electrons, respectively, as discussed above.

As $h\nu$ increases from 22 eV to 92 eV, the intensity near E_F increases and then decreases with respect to that of the Ni $3d$ main peak. The former trend reflects the increasing U $5f$ emission near E_F that has a maximum around $h\nu \sim 50$ eV. The latter trend is due to the suppression of the U $5f$ emission at $h\nu = 92$ eV (U $5d \rightarrow 5f$ off resonance) as well as the decreasing Sn sp and U $6d$ emission relative to the Ni $3d$ emission with increasing $h\nu$.¹⁶ Thus this observation indi-

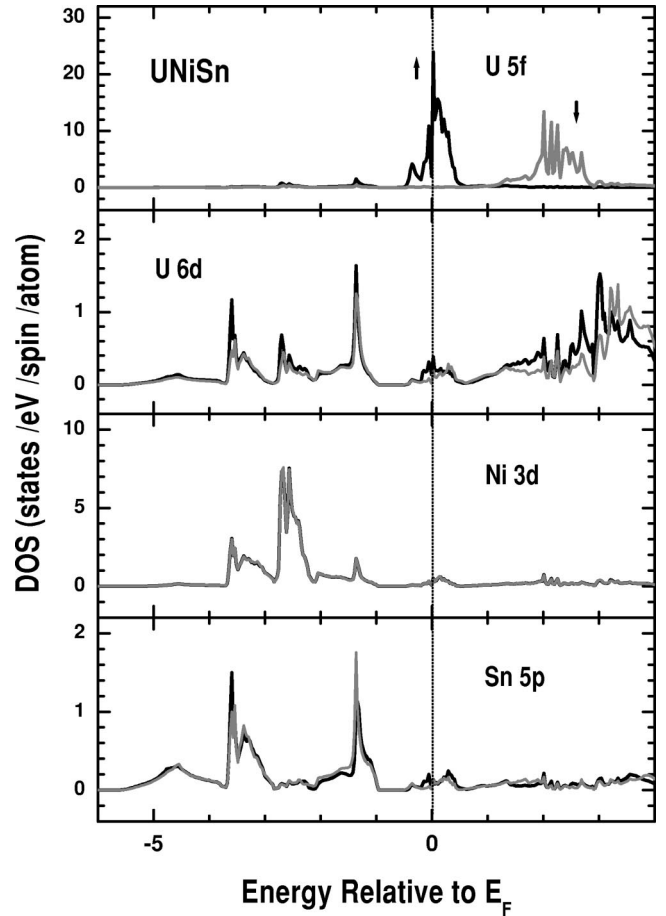


FIG. 3. Projected angular momentum density of states (PLDOS), obtained from the LSDA calculation for the AF ground state of UNiSn. From the top, PLDOS per spin and per atom of U $5f$, U $6d$, Ni $3d$, and Sn $5p$ electrons, respectively. The spin-up PLDOS are denoted by black lines and the spin-down PLDOS are denoted by grey lines.

cates that the electronic states near E_F have a dominant U $5f$ electron character, but hybridized with the U $6d$ and Sn sp states. Indeed this conclusion is consistent with our band structure calculation, which will be shown in Fig. 3.

Figure 2(a) presents the extracted U $5f$ PSW (dots), corresponding to the difference between the U $5d \rightarrow 5f$ on-resonance spectrum (solid line) and off-resonance spectrum (dashed line). The U $5f$ spectrum exhibits a pronounced peak centered at about 0.3 eV BE with a FWHM of ~ 1.4 eV and a tail to about 3 eV below. It is reminiscent of the U $5f$ PSW's of other U intermetallic compounds in having much spectral weight around E_F and showing the broad $5f$ width.^{15,19–23} The U $5f$ spectrum shows a change in the slope around 2 eV BE, the intensity of which depends on the scale factor. The off-resonance spectrum is multiplied by a scale factor to account for the $h\nu$ dependence of other conduction-band electrons. Therefore the existence of the 2 eV feature seems to be within experimental uncertainty. The U $6d$ emission is known to resonate at the $5d$ absorption edge as well.²¹ There is uncertainty in the resonant strength of the $6d$ states with respect to that of the $5f$ states in uranium compounds.²¹ Further, the line shape of the U $6d$ PSW

is not known for UNiSn yet. However, it is likely that the resonating U $6d$ intensity is normalized out in subtracting the off-resonance spectrum from the on-resonance spectrum because it usually mimics the ligand d and sp DOS. In other words, the U $6d$ wave functions overlap substantially with the Ni $3d$ wave functions in space and energy, resulting in a large hybridization between them. The $h\nu$ range employed in this study is surface sensitive, and so it is also possible that the surface $5f$ emission might contribute to the region around 2–3 eV BE, as found in Ce systems.^{24,25} On the other hand, surface effects have not been observed explicitly in uranium systems,²³ in contrast to Ce systems for which surface effects have been well established.

The extracted $5f$ PSW of UNiSn is compared to those of UAl_2 (Ref. 20) and UPd_3 (Ref. 22) in Fig. 2(b). All the spectra are scaled at the peak. UAl_2 and UPd_3 are classified as a nearly-heavy-fermion system and a typically localized $5f$ system, respectively. The peak in UPd_3 is known to correspond to the $5f^2 \rightarrow 5f^1$ transition of U^{4+} ions,²² while the $5f$ peak close to E_F in UAl_2 corresponds to the fully relaxed $5f^n c^{m-1}$ final states ($n=2, 3, 4$), where the $5f^n c^m$ ground-state configuration is assumed. In the local density-functional approximation (LDA) band theoretical view, the $5f$ peak near E_F is interpreted as the ground-state U $5f$ band. It is observed that, as one moves from UAl_2 to UNiSn and UPd_3 , the centroid of the $5f$ electron peak moves away from E_F and its width becomes wider, resulting in a decreasing $5f$ DOS at the E_F , $N_f(E_F)$, from UAl_2 to UNiSn and UPd_3 . This trend is similar to that in the $Y_{1-x}U_xPd_3$ system,²² indicating that the direct f - f hopping among the U $5f$ electrons decreases from UAl_2 to UNiSn and UPd_3 .

In contrast to the large $5f$ spectral weight around E_F in UAl_2 , UNiSn reveals a reduced $5f$ -electron weight around E_F because the $5f$ -electron peak is located farther away from E_F and the $5f$ width is wider than in UAl_2 . This difference between UNiSn and UAl_2 might be understood by the fact that the average U-U separation in UNiSn ($d=4.53$ Å) is quite large, larger than that in UAl_2 ($d=3.22$ Å) and even larger than the Hill limit ($d_{Hill}=3.3$ – 3.5 Å),²⁶ beyond which the U $5f$ electrons are observed to form local moments, suggesting that the direct interaction between near-neighbor U $5f$ electrons is negligible in UNiSn. It is consistent with the fact that UNiSn has a large ordered magnetic moment of $1.55\mu_B$ obtained from a neutron diffraction study.¹ This value is significantly large, as compared to other U intermetallic systems. An inelastic neutron scattering study done by one of us also found rather well-defined CEF excitations in UNiSn.⁸ Thus the interaction between U $5f$ electrons in UNiSn should be mediated by hybridization to conduction-band electrons, such as U $6d$, Sn sp , and Ni $3d$ electrons.

Note that the average hybridization strength between U $5f$ and Ni $3d$ /Sn sp electrons is expected to be large in UNiSn. The U-Ni separation (2.77 Å) is very small, even smaller than the U-Sn separation (3.20 Å) and the U-Al separation in UAl_2 (3.22 Å), suggesting a large hybridization between U $5f$ and Ni $3d$ electrons in UNiSn. Thus a possible explanation for the reduced $N_f(E_F)$ in UNiSn is that

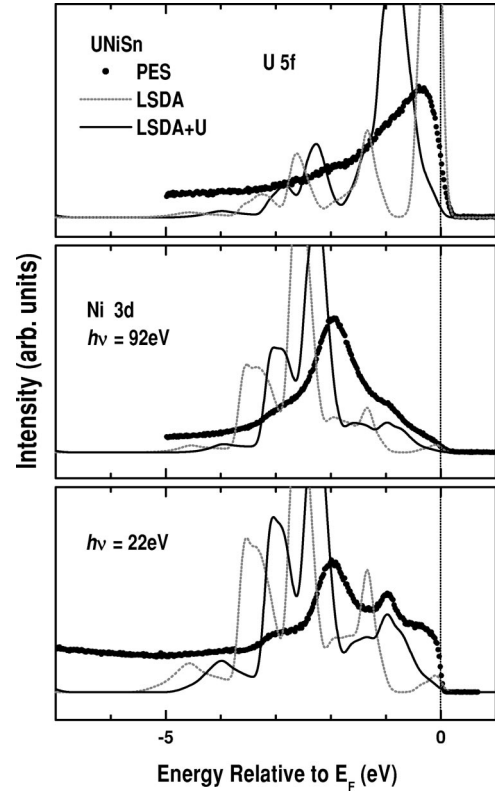


FIG. 4. Top: comparison of the extracted U $5f$ PSW of UNiSn (dots) to the calculated PLDOS, obtained from the LSDA calculation (dotted line) and from the LSDA+ U calculation (solid line). In this comparison only the occupied part of the PLDOS is taken, and then convoluted by a Gaussian function with 0.2 eV at FWHM to simulate the instrumental resolution. Middle: similarly for Ni $3d$ states. Bottom: comparison of the $h\nu=22$ eV PES spectrum of UNiSn (dots) to the sum of the U $6d$, Ni $3d$, and Sn $5p$ PLDOS. See the text for details.

the virtual charge fluctuations leading to a large $N_f(E_F)$ are suppressed by a small Ni d DOS at E_F via hybridization. To obtain a solid picture of the hybridization interaction in UNiSn, it will be necessary to calculate the hybridization matrix elements.

B. Comparison to the LSDA and LSDA+ U calculation

Figure 3 shows the PLDOS of UNiSn, obtained from the LSDA calculation by assuming an AF ground state. Each PLDOS is per atom, and the spin-up and spin-down PLDOS are denoted by black and gray lines, respectively. It is shown that the valence band extends from E_F to about 5 eV below E_F , in agreement with the measured photoemission spectra (see Figs. 1 and 4). The U f states exhibit exchange-split bands, separated by about 2–2.5 eV from each other. The other states (U d , Ni d , Sn p) exhibit nearly no exchange splitting, indicating that the spin polarization in UNiSn is mainly due to U $5f$ electrons. In consequence, the calculated spin magnetic moment of U is $2.40\mu_B$, while the magnetic moment of Ni is negligible. The Fermi level lies in the middle of the spin-up U f bands that are hybridized with the U d , Ni d , and Sn p states. Much of the spin-up f states are

concentrated within ± 0.5 eV from E_F . The Ni d bands are nearly filled with a very low DOS at E_F , in agreement with the very low spectral intensity in the Ni 3d PSW (see the $h\nu=92$ eV spectrum in Fig. 1). Most of the Sn p states are concentrated at 1–5 eV below E_F , resulting in a small DOS near E_F . Therefore the largest contribution to $N(E_F)$ comes from the U f electrons ($\sim 85\%$) with a small contribution from U $6d$ ($\sim 6\%$), Ni $3d$ ($\sim 7\%$), and Sn sp ($\sim 2\%$) electrons. The U d , Ni d , and Sn p bands are much wider than the U f bands, consistent with the negligible exchange splitting in these bands. The U d , Ni d , and Sn p PLDOS share common features, indicating a large hybridization among them. These theoretical results are qualitatively similar to those of previous reports.^{9,27} The AF phase of UNiSn corresponds to a normal metal, in contrast to the half-metallic nature of the ferromagnetic phase of UNiSn.²⁷

Figure 4 compares the extracted PSW's of UNiSn to the calculated PLDOS, obtained from the LSDA (dotted lines) and LSDA+ U (solid lines) calculations, respectively. In comparison to the PES spectra, only the occupied part of the calculated PLDOS was taken, and then convoluted by a Gaussian function with 0.2 eV at the FWHM. The Gaussian function has been used to simulate the instrumental resolution. The effects of the lifetime broadening and photoemission matrix elements are not included in the theory curves. In the bottom panel, the theoretical spectrum was obtained by adding the U d , Ni d , and S p PLDOS, because none of the contributions are negligible at $h\nu=22$ eV and it is difficult to separate out the different electron emissions (see the discussion under Fig. 1). The LSDA calculation shows a large discrepancy with experiment even though the calculated bandwidths are comparable to the measured valence-band widths. The most pronounced discrepancy is that the calculated peak positions in the Ni d and Sn p PLDOS appear at higher BE's than in the PES spectra by more than 0.5 eV. As to the U f states, the experimental 5f PSW shows extra intensity from ~ 0.5 eV to about 3 eV BE with respect to the LSDA calculation, for which much of the occupied f PLDOS is concentrated within 0.5 eV from E_F . Further, the experimental 5f PSW shows a reduced 5f weight at E_F in contrast to the high $N_f(E_F)$ in the LSDA.

In order to examine the origin of such disagreement between experiment and the LSDA, the on-site Coulomb correlation parameter U for the U 5f electrons has been incorporated in the electronic structure calculation for UNiSn. The parameters used in this calculation are the Coulomb correlation $U=2.0$ eV and the exchange $J=0.95$ eV. In the LSDA+ U calculation, the on-site Coulomb correlation for the Ni 3d electrons has been neglected because including the Ni d Coulomb correlation in the LSDA+ U calculation makes the discrepancy between experiment and theory worse.²⁸ As in the previous report,⁹ the LSDA+ U correctly yields the correct metallic ground state for the AF phase of UNiSn and the semiconducting state for the PM phase of UNiSn. The calculated spin and orbital magnetic moments for U are $2.25\mu_B$ and $-4.53\mu_B$, respectively, and so the total magnetic moment of U becomes $2.28\mu_B$. This value is in reasonable agreement with experiment¹ and the previous report.⁹

The effect of including the on-site Coulomb interaction between the U 5f orbitals in the LSDA+ U is the shift of the occupied 5f peak below E_F toward a higher BE and the shift of the unoccupied 5f peak above E_F farther away from E_F . The second effect of the LSDA+ U is the shift of the U d , Ni d , and Sn p PLDOS toward E_F , namely, toward lower BE's. The larger the value of U is employed, the larger the shifts in the peaks of the U 5f, 6d, Ni d , and Sn p PLDOS become. The latter effect of the LSDA+ U calculation produces better agreement with the measured PES spectra. In particular, the 1 eV peak (B) (of U 6d–Sn 5p hybridized electron character) and the 2 eV peak (C) (predominantly of Ni 3d electron character) in the PES spectra exhibit good agreement with the LSDA+ U (solid lines), compared to the LSDA (dotted lines). This finding certainly suggests the importance of the on-site Coulomb interaction between U 5f electrons in determining the electronic structure of UNiSn. In contrast, the LSDA+ U calculation does not improve the U f PLDOS: (i) the calculated f peaks in the occupied part appear at higher BE's than in experiment, and (ii) the calculated $N_f(E_F)$ becomes too small. A smaller value of U would yield an improved agreement with the experimental U 5f PSW, but then it would yield a larger discrepancy with the other conduction-band features of the Ni d , U d , and Sn p electrons. Therefore neither the LSDA nor the LSDA+ U seems to provide a consistent description of the experimental electronic structure of UNiSn at the moment.

C. Temperature dependence in PES

Figure 5 compares the normalized valence-band photoemission spectrum of UNiSn obtained at $T=15$ K (dots), which belongs to the AF metallic phase, to that at $T=90$ K (solid line) which belongs to the paramagnetic semiconducting phase. The top and bottom panels show the spectra obtained at $h\nu=22$ eV and $h\nu=98$ eV, respectively. The inset compares the $h\nu=22$ eV spectra, after the inelastic backgrounds have been subtracted in a standard way. Our data in Fig. 5 reveal the following features. (i) Essentially no T -dependent changes are observed in the large-energy-scale line shapes. Upon heating, there is a small transfer of spectral weight from lower BE (between E_F and 1 eV BE) to higher BE (>3 eV BE). This change might indicate a reduced DOS at E_F in the semiconducting phase. (ii) Peak locations do not change with T , indicating that the Fermi level stays unchanged in both the AF metallic phase and the paramagnetic semiconducting phase. (iii) The metallic Fermi edge is still observed above T_N ($T=90$ K $>$ $T_N \approx 43$ K), which seems to be contradictory to the SM transition inferred from other experiments for UNiSn.

Figure 6 shows the T dependence of the high-resolution PES spectrum of UNiSn in the vicinity of E_F . All the spectra were obtained with the same measurement conditions except for temperature. The top panel compares the high-resolution PES spectrum of UNiSn obtained at $T=15$ K (dots) to that obtained at $T=90$ K (solid line), taken at $h\nu=22$ eV. The middle panel compares the $T=15$ K spectrum of UNiSn (dots) to that of Pt metal (solid line), both with FWHM ≈ 30 meV. In this comparison, two spectra are scaled to

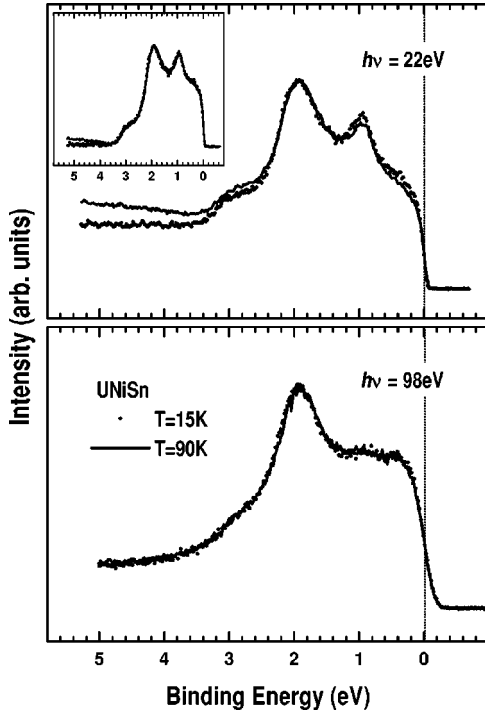


FIG. 5. (a) Comparison of the T -dependent valence-band PES spectra of UNiSn at $h\nu=22$ eV below T_N ($T=15$ K) and above T_N ($T=90$ K). Inset: comparison of the two spectra after the inelastic backgrounds are subtracted. (b) Comparison of the T -dependent valence-band PES spectra of UNiSn at $h\nu=98$ eV for $T=15$ K and $T=90$ K.

each other at about 300 meV below E_F . Superposed on the $T=15$ K PES spectrum of UNiSn is the V-shaped metallic DOS that is cut off at E_F by the 15 K Fermi distribution function and convoluted with a Gaussian function of FWHM=30 meV. We have employed the V-shaped metallic DOS because it is usually formed in semimetallic systems. The dotted line along the measured spectrum of Pt metal is the result of the flat DOS with a nonzero slope, cut off at E_F by the 15 K Fermi function and convoluted with a Gaussian function. The bottom panel shows the $T=90$ K PES spectrum of UNiSn (dots), compared to the same V-shaped metallic DOS (gray line). The model DOS is now multiplied by the 90 K Fermi function and convoluted with a Gaussian function (solid line).

Figure 6 provides the following information. (i) Nearly no change has been observed in the PES spectrum of UNiSn with temperature (see the top figure), except that due to the temperature broadening, as confirmed in the analysis shown in the lower panels. This observation is quite puzzling because it suggests that there is no appreciable change in the electronic structure of UNiSn across T_N , in spite of the novel phase transitions across T_N . (ii) The slope of the high-resolution PES spectrum of UNiSn just below E_F is lower than that of Pt. In contrast to the simple linear DOS for Pt (a flat DOS with a nonzero slope), the 15 K spectrum of UNiSn is described well by the V-shaped metallic DOS near E_F (a model with a reduced but finite DOS at E_F). This difference suggests that UNiSn has a low $N_f(E_F)$, even though there is

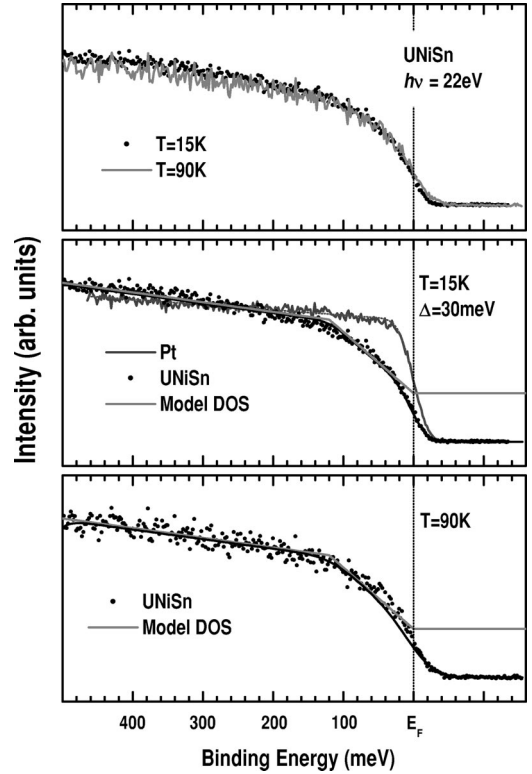


FIG. 6. Top: Comparison of high-resolution photoemission spectra of UNiSn in the vicinity of E_F at $T=15$ K and $T=90$ K, taken at $h\nu=22$ eV with FWHM ~ 30 meV. Middle: the $h\nu=22$ eV spectrum of UNiSn at $T=15$ K (dots), compared to that of Pt metal (solid line). Superposed on the PES spectrum of UNiSn is the V-shaped metallic DOS that is multiplied by a 15 K Fermi function and convoluted with a Gaussian function of FWHM = 30 meV (solid line). Bottom: similarly for the $h\nu=22$ eV spectrum at $T=90$ K.

certainly a finite metallic DOS at E_F in UNiSn. We interpret this reduction in $N_f(E_F)$ as due to the very low DOS of the Ni 3d PLDOS in UNiSn. That is, the reduced $N_f(E_F)$ is caused via the energy-dependent hybridization matrix element between the U 5f states that are located away from E_F and the Ni 3d states that have the main peak well below E_F (about 2 eV BE) and a very low DOS at E_F . (iii) The same V-shaped metallic DOS provides a reasonably good fit to the measured 90 K spectrum. Further, it is found that the model with a real gap or a pseudogap²⁹ of width 10 meV below E_F cannot describe the measured $T=90$ K PES spectrum of UNiSn.³⁰ These findings indicate that UNiSn has a finite metallic DOS at E_F above T_N .

Finally, we would like to discuss the origin of no appreciable difference being observed in the spectra between $T=15$ K and $T=90$ K. Since our photoemission data are surface sensitive as mentioned previously, it is possible that the surface emission can cause the observed T -invariant spectral features near E_F . If the surface layers did not go through the SM transition with temperature or if there were impurity phases on the surface, the possible T -dependent variation of the spectral features could be smeared. On the other hand, our data do not eliminate the possibility of the opening of an

anisotropic gap²⁹ of size smaller than <5 meV at $T > T_N$, considering the experimental resolution achieved in this work. The size of the gap (<5 meV) compatible with our high-resolution PES data is much smaller than that suggested by other experiments (67–76 meV).³ This situation for UNiSn is similar to that for CeNiSn.¹⁷ Our experiment does not allow us to determine the anisotropic electronic structure of UNiSn, because the sample is polycrystalline and so the spectra are effectively angle integrated. To check this, it is necessary to do angle-resolved PES measurements for single-crystalline UNiSn, which is not available at the present time.

IV. CONCLUSIONS

The electronic structure of UNiSn has been investigated by performing a photoemission experiment and electronic structure calculation in the LSDA and LSDA+ U methods. The $h\nu$ dependence of the valence-band spectrum reveals that the electronic states at E_F have a dominant U 5*f* electron character. The U 5*f* PSW exhibits a broad peak centered at ≈ 0.3 eV BE with a FWHM of ~ 1.4 eV, extending to about 3 eV below. The U 5*f* PSW of UNiSn is compared to those of UAl₂ and UPd₃. The centroid of the 5*f* electron peak moves away from E_F from UAl₂ to UNiSn and UPd₃, indicating that direct *f-f* hopping decreases from UAl₂ to UNiSn and UPd₃. Its width becomes wider in UNiSn than in UAl₂, reflecting the large hybridization between U 5*f* and Ni 3*d* electrons in UNiSn. The LSDA+ U calculation yields better agreement with the measured PES spectra than the LSDA calculation, suggesting that the on-site Coulomb interaction between 5*f* electrons is important in determining the electronic structure of UNiSn. However, neither the

LSDA+ U nor the LSDA provides a consistent description of the measured U 5*f* PES spectra of UNiSn, suggesting that the LSDA+ U method does not properly account for the effect of the U 5*f* Coulomb correlation in UNiSn. The Sn *sp* and U 6*d* states are found to spread over the whole valence band, i.e., from E_F to ~ 4 eV below, with a very low spectral weight near E_F . In the Ni 3*p*→3*d* RPES, a satellite feature has been observed about 6 eV below the Ni 3*d* main band, indicating a non-negligible Ni 3*d* Coulomb correlation in UNiSn.

The high-resolution photoemission spectrum of UNiSn shows a lower slope just below E_F than that of Pt, and is described well by a V-shaped metallic DOS near E_F , implying a reduced 5*f* DOS at E_F in UNiSn. A possible mechanism for such a reduction in $N_f(E_F)$ might be the hybridization to the Ni 3*d* states that have a very low DOS at E_F . The T -dependent high-resolution PES of UNiSn reveals essentially no changes with T and a finite DOS at E_F both below and above T_N , suggesting a semimetallic electronic state for $T > T_N$. Our data do not eliminate the formation of the pseudogap of width <5 meV for $T > T_N$, and the contribution from the T -invariant surface emission near E_F .

ACKNOWLEDGMENTS

We are grateful to S.-J. Oh and E.-J. Cho for helpful discussions. This work was supported by the Center for Strongly Correlated Materials Research (CSCMR) at SNU and the electron Spin Science Center (eSSC) at POSTECH. One of us (J.G.P.) acknowledges support by the Korean Research Foundation (Grant No. KRF-2000-015-DP0111). The SRC is supported by the NSF (DMR-0084402).

¹H. Kawanaka, H. Fujii, M. Nishi, T. Takabatake, K. Motoya, Y. Uwatoko, and Y. Ito, J. Phys. Soc. Jpn. **58**, 3481 (1989).

²T.T.M. Palstra, G.J. Nieuwenhuys, R.F.M. Vlastuin, J. van den Berg, J.A. Mydosh, and K.H.J. Buschow, J. Magn. Magn. Mater. **67**, 331 (1987).

³H. Fujii, H. Kawanaka, T. Takabatake, M. Kurisu, Y. Yamaguchi, J. Sakurai, H. Fujiwara, T. Fujita, and I. Oguro, J. Phys. Soc. Jpn. **58**, 2495 (1989).

⁴J. Diel, H. Fischer, R. Köhler, C. Geibel, F. Steglich, Y. Maeda, T. Takabatake, and H. Fujii, Physica B **186-188**, 708 (1993).

⁵T. Akazawa, T. Suzuki, F. Nakamura, T. Fujita, T. Takabatake, and H. Fujii, J. Phys. Soc. Jpn. **65**, 3661 (1996).

⁶Y. Aoki, T. Suzuki, T. Fujita, H. Kawanaka, T. Takabatake, and H. Fujii, Phys. Rev. B **47**, 15 060 (1993).

⁷T. Akazawa, T. Suzuki, H. Goshima, T. Tahara, T. Fujita, T. Takabatake, and H. Fujii, J. Phys. Soc. Jpn. **67**, 3256 (1998); T. Akazawa, T. Suzuki, T. Tahara, T. Goto, J. Hori, H. Goshima, F. Nakamura, T. Fujita, T. Takabatake, and H. Fujii, Physica B **259-256**, 248 (1999).

⁸K.A. McEwen, M.J. Bull, and R.S. Eccleston, Physica B **281-282**, 600 (2000).

⁹P.M. Oppeneer, A.N. Yaresko, A.Ya. Pelov, V.N. Antonov, and H. Eschrig, Phys. Rev. B **54**, R3706 (1996).

¹⁰H. Höchst, K. Tan, and K.H.J. Buschow, J. Magn. Magn. Mater. **54-57**, 545 (1986).

¹¹V.I. Anisimov, F. Aryasetiawan, and A.I. Liechtenstein, J. Phys.: Condens. Matter **9**, 767 (1997).

¹²The 6 eV BE emission in the valence-band spectrum indicates the oxygen contamination of the measured surface.

¹³The 9.5 eV peak is known to be due to CO (carbon-monoxide) adsorbed on the surface or defects at the grain boundaries. See J.-S. Kang, Y.J. Kim, B.W. Lee, C.G. Olson, and B.I. Min, J. Phys.: Condens. Matter **13**, 3779 (2001).

¹⁴S.K. Kwon and B.I. Min, Phys. Rev. Lett. **84**, 3970 (2000).

¹⁵A.J. Arko, C.G. Olson, D.M. Wieliczka, Z. Fisk, and J.L. Smith, Phys. Rev. Lett. **53**, 2050 (1984).

¹⁶J.J. Yeh and I. Lindau, At. Data Nucl. Data Tables **32**, 1 (1985).

¹⁷J.-S. Kang, C.G. Olson, Y. Inada, Y. Ōnuki, S.K. Kwon, and B.I. Min, Phys. Rev. B **58**, 4426 (1998).

¹⁸S. Hüfner and G.K. Wertheim, Phys. Lett. **51A**, 299 (1975); **51A**, 301 (1975).

¹⁹J.W. Allen, S.-J. Oh, L.E. Cox, W.P. Ellis, M.S. Wire, Z. Fisk, J.L. Smith, B. Pate, I. Lindau, and A.J. Arko, Phys. Rev. Lett. **54**, 2635 (1985).

- ²⁰J.-S. Kang, J.W. Allen, M.B. Maple, M.S. Torikachlivi, B. Pate, W.P. Ellis, and I. Lindau, *Phys. Rev. Lett.* **59**, 493 (1987).
- ²¹A.J. Arko, D.D. Koelling, C. Capasso, M. del Giudice, and C.G. Olson, *Phys. Rev. B* **38**, 1627 (1988).
- ²²J.-S. Kang, J.W. Allen, M.B. Maple, M.S. Torikachlivi, W.P. Ellis, B. Pate, Z.-X. Shen, J.J. Yeh, and I. Lindau, *Phys. Rev. B* **39**, 13 529 (1989).
- ²³J.W. Allen, Y.-X. Zhang, L.H. Theng, L.E. Cox, M.B. Maple, and C.-T. Chen, *J. Electron Spectrosc. Relat. Phenom.* **78**, 57 (1996).
- ²⁴L. Duo, *Surf. Sci. Rep.* **32**, 233 (1998).
- ²⁵A. Sekiyama, T. Iwasaki, K. Matsuda, Y. Saitoh, Y. Onuki, and S. Suga, *Nature (London)* **403**, 398 (2000).
- ²⁶H. H. Hill in *Plutonium 1970 and Other Actinides*, Nuclear Metals Vol 17, edited by W. N. Miner (AIME, New York, 1970), pp. 2–19.
- ²⁷R.C. Albers, A.M. Boring, G.H.I. Daalderop, and F.M. Mueller, *Phys. Rev. B* **36**, 3661 (1987).
- ²⁸The main effect of including the on-site Coulomb interaction between the Ni 3*d* orbitals in the LSDA+*U* is pushing the occupied part of the Ni 3*d* bands farther away from E_F (toward a higher BE) and the narrowing of the bandwidth. This causes a larger discrepancy with experiment.
- ²⁹The pseudogap or the anisotropic gap denotes a V-shaped DOS with a residual flat DOS below E_F , corresponding to the anisotropic gap that exists over only part of the Fermi surface.
- ³⁰J.-S. Kang (unpublished).